JOURNAL OF SYNCHROTRON RADIATION
ISSN 1600-5775

Pump–probe laser system at the FXE and SPB/SFX instruments of the European X-ray Free-Electron Laser Facility[1]

Guido Palmer, Martin Kellert, Jinxiong Wang, Moritz Emons, Ulrike Wegner, Daniel Kane, Florent Pallas, Tomasz Jezynski, Sandhya Venkatesan, Dimitrios Rompotis, Erik Brambrink, Balazs Monoszlai, Man Jiang, Joachim Meier, Kai Kruse, Mikhail Pergament and Max J. Lederer*

European XFEL, Holzkoppel 4, Schenefeld 22869, Germany. *Correspondence e-mail: max.lederer@xfel.eu

Received 9 October 2018
Accepted 18 January 2019

Edited by P. Fuoss, SLAC National Accelerator Laboratory, USA

[1] This article will form part of a virtual special issue on X-ray free-electron lasers.

Keywords: ultrafast lasers; burst-mode laser; X-ray FEL.

User operation at the European X-ray Free-Electron Laser Facility started at the SASE1 undulator beamline in fall 2017. The majority of the experiments utilize optical lasers (mostly ultrafast) for pump–probe-type measurements in combination with X-ray pulses. This manuscript describes the purpose-developed pump–probe laser system as installed at SASE1, implemented features and plans for further upgrades.

1. Introduction

The European XFEL (EuXFEL) was built with the objective to provide ultrafast X-ray pulses with ultimate brightness for user experiments. In addition, at the EuXFEL, the experimental data-taking efficiency is increased markedly by upscaling the number of pulses per second to a maximum of 27 000. This value is more than two orders of magnitude higher than that of other operating hard X-ray free-electron laser (FEL) facilities. The high pulse rate of the EuXFEL is quite specific though. Owing to the burst-mode operation of the accelerator, X-ray femtosecond pulses are emitted in 10 Hz bursts for durations up to 600 µs and with up to 2700 pulses per burst, *i.e.* up to 4.5 MHz within the bursts. For further details about this operation mode, refer to the work by Altarelli (2006) and Tschentscher *et al.* (2017). In order to maximally exploit the experimental capabilities of the EuXFEL, the ultrafast optical pump–probe laser (PP laser) should also work in burst mode and employ advance pulse-selection technology in order to be compatible with the emission pattern of the FEL.

The SASE1 instruments Femtosecond X-ray Experiments (FXE; Bressler *et al.*, 2019) and Single Particles, Clusters, and Biomolecules and Serial Femtosecond Crystallography (SPB/SFX; Mancuso *et al.*, 2019) have laser parameter requirements quite typical for an ultrafast PP laser, at least when considered in isolation. Apart from burst operation, these are ultrashort pulse durations ranging from a few optical cycles to hundreds of fs, a repetition rate up to 4.5 MHz, pulse energies of a few µJ to tens of mJ, pulse-on-demand (PoD), synchronization with low jitter/drift, and extensions to different wavelengths ranging from the UV to mid-IR and THz. Viewed in combination, there is no commercial vendor offering a laser system with such parameters. As a result, the EuXFEL engaged in a laser development project to address the requirements in

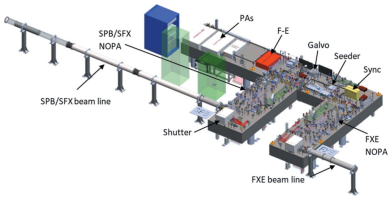

combination with the need for high laser up-time during operation (goal: >95%).

Generating mJ-level fs pulses at MHz repetition rates equates to kW-level average power during a burst. To enable such performance, combined with the above-listed features, several fundamental technology selections needed to be made early and followed through with in-house and collaborative industry developments lasting several years. The most important decisions are the following: (i) The 800 nm broadband pulses are amplified in a multi-stage non-collinear optical parametric amplifier (NOPA) rather than Ti:sapphire technology. (ii) For the sophisticated pump amplifiers needed for the NOPAs, preference was given to Yb:YAG-based InnoSlab technology over thin-disk, fibre- or cryo-technology. (iii) The custom-developed burst-mode chirped pulse amplification (CPA) front-end amplifier (F-E) for the synchronized generation of NOPA-signals and pump amplifier (PA) seed pulses is entirely Yb-fibre based. This leads to enhanced flexibility compared with regenerative amplifier technology. The desired intra-burst frequencies are set in the F-E. They also determine the NOPA pulse energies. (iv) Origami 10 seed oscillators (OneFive GmbH) are chosen for their ultralow jitter and the tested interface with the Deutsches Elektronen-Synchrotron (DESY) and EuXFEL synchronization system (Müller *et al.*, 2018). Most of the laser-related development results can be found in the literature (Pergament *et al.*, 2014, 2016, and references therein).

Starting in 2011 with the establishment of the Optical Lasers group at EuXFEL, followed by first design studies, buildup of an R&D lab and first experiments in 2012, the development of a prototype PP laser was finalized in 2016. Concurrent CAD design of production systems, procurement of components and finalization of the PP laser room at SASE1 enabled the start of installation in fall 2016. In the following sections, we will introduce the laser design and beam delivery to FXE and SPB/SFX at SASE1. Current available features and upgrade plans for the near future are also presented.

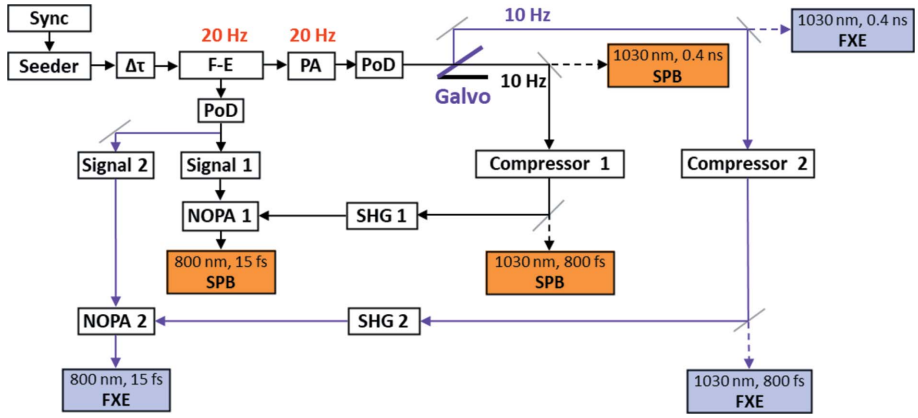

Figure 1
Conceptual design of the SASE1 PP laser. A synchronized seed oscillator (Origami 10) provides input to the CPA F-E with timing-locked output bursts at 20 Hz for signal generation (supercontinuum) and pump amplification in the PA. Pulse pickers for pump and signal beams enable intra-burst PoD. De-multiplexing (Galvo) results in two pump bursts at 10 Hz, which are converted to the second harmonic (SHG) to drive two independent NOPAs – one for FXE, the other for SPB/SFX. Apart from the 800 nm broadband beamline, the instruments can also receive the compressed or uncompressed 1030 nm pump.

2. SASE1 pump–probe laser design and beam delivery

The laser concept, which finally came to realization at SASE1, is shown schematically in Fig. 1. One challenge for the final installation of a production system at SASE1 was the need for simultaneous laser operation at the two instruments of SASE1. For instance, while only one instrument receives X-rays together with the timed PP laser during a given shift, laser-related setup work at the other instrument should be possible in parallel and with parameters relevant for their following X-ray shift. Yet, for space and cost reasons, there is only one F-E and PA in the PP laser room. This was solved by the process illustrated in Fig. 1. The F-E and PA systems are operated at a 20 Hz burst repetition rate. The resulting pump bursts are then temporally de-multiplexed and spatially separated using a galvo-scanner, which results in two 10 Hz pump beamlines. Each instrument has a dedicated NOPA setup, and the instrument that receives X-rays also receives the correspondingly timed laser burst. The other instrument ideally receives the bursts as required during their upcoming X-ray shift, but timed 50 ms off the X-ray.

Fig. 2 shows the CAD integration of the PP laser as implemented in the SASE1 laser hutch (covers off). The F-shaped table system is surrounded by clean room curtains (not shown), inside of which the air conditioning system provides ISO 5 air quality and ±0.1°C temperature and ±2.5% humidity stability.

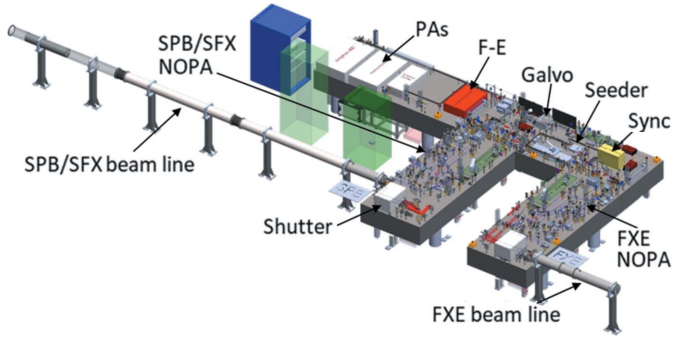

Figure 2
CAD-rendering of the SASE1 PP laser. The F-shaped table system hosts the separate NOPAs on the arms of the F. Main components are annotated. To minimize the *B* integral, the beam pipes carry low-grade vacuum (0.5 mbar) and the beams are large (25 mm) at the entrance and exit windows. There is one port each for 800 nm and 1030 nm beams. To minimize the impact of environmental influences on the beam transport, the vacuum beamlines are free of mirrors and lenses. Relay imaging through the pipes is implemented with curved mirrors where necessary.

The PP laser rooms in the experiment hall of EuXFEL are shown in Fig. 3. Note that beams are transported to the respective instrument laser hutch (ILH) first. There, various operations can be performed such as attenuation, wavelength conversion, delay scans, *etc*. before the beam is finally transported to the experiment. The advantage of this separation is an enhanced stability of the laser source, as the PP laser hutch is typically not entered during a user run. Also, work in the ILHs can continue independently of X-ray operation. As for the planned THz and timing-tool setups, these will be placed directly in the experiment rooms.

Control and monitoring of the PP laser is achieved via the newly developed EuXFEL photon system control system 'Karabo' (Hauf *et al.*, 2019). A large number of important laser parameters and settings can be viewed/changed online, and a switch between shifts can be performed remotely. There is also a long-term data logging capability. Ideally, the PP laser is prepared for an experiment during the preceding setup days in such a way that all experimental requirements of both instruments can be covered with one basic laser set point (see Section 3). All changes necessary during the run (attenuation, patterns, *etc*.) are then carried out remotely or in the ILH or experiment hutch. This includes tools to shift the arrival time of PP laser pulses relative to the X-ray pulses to find temporal overlap and perform pump–probe scans. Ultimately, this mode of operation will guarantee highest laser stability and up-time and will maximize the time for data-taking during one 12 h shift.

Experience to date shows that the average power stability of the NOPAs is better than 10% (without correction) over the course of a five-day run with shifts changing every 12 h. This is assuming that the air conditioning system is operating within specifications and that all active drift stabilization loops are closed. Similar performance is achieved with respect to far-field pointing drift and jitter, *i.e.* <10% r.m.s. of the beam diameter at the focus.

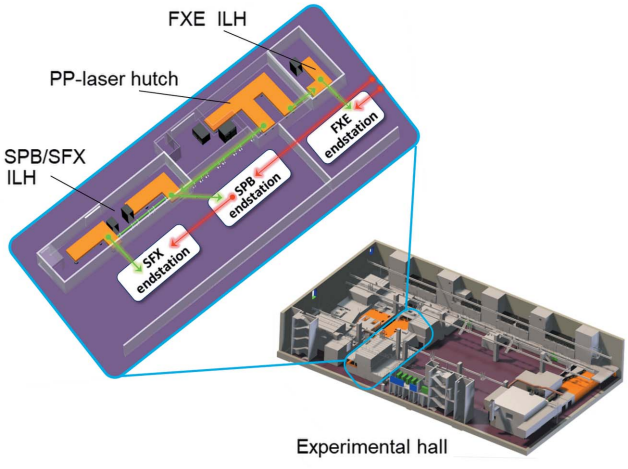

Figure 3
The layout of the experiment hall with locations of PP laser rooms at SASE1, 2 and 3 marked in orange. Instrument laser hutches (ILH) receive the two beamlines (800 nm and 1030 nm) of the PP laser (green arrows). Operations such as attenuation, wavelength conversion, delay scans, *etc*., can be performed there, while the PP laser hutch need not be entered, which enhances the stability of the source. A timing tool and THz setup will be placed in the experiment rooms.

Table 1
The PP laser set points.

For 2 and 3, limited variations of the repetition rates are possible (around 1 MHz and 200 kHz). The stated pulse energies refer to operation exclusively in one of the two wavelengths and as measured at the exit of the PP laser hutch. The level of average power during a burst is 4 kW (1030 nm) and 300 W (800 nm). The corresponding burst energies, *e.g.* at a 300 µs burst duration, are 1.2 J and around 100 mJ, respectively. There is also the possibility for a mixed mode. In this case, a high repetition rate NOPA set point (1 or 2) is pumped at a lower frequency and the spare pump pulse energy can be passed to the experiment (compressed or uncompressed). This mode corresponds to a two-colour synchronized PP laser operation.

Set point	Repetition rate (MHz)	E1030 nm (mJ)	NOPA stages	E800 nm (mJ)
1	4.5	1	I+II	0.05
2	1.13	4	I+II	0.3
3	0.188	21	I+II+III	1.5
4	0.1	40	I+II+III	2.5

The PP laser seed oscillator is synchronized to the ultra-stable low-noise EuXFEL mode-locked Master Laser Oscillator (MLO), which is again phase-locked to the RF Master Oscillator (MO). Its pulses are distributed via actively length-stabilized optical fibres to the different locations across the accelerator and endstations, requiring synchronization. At the PP laser, the synchronization to the optical reference is based on a PLL-type (phase-locked loop) phase-detection scheme at the 25th harmonic (1354 MHz) of the oscillator repetition rate. An in-loop jitter of <30 fs r.m.s. is measured in this case. Once combined with the all-optical two-colour balanced optical cross-correlation scheme to precisely measure the timing error between the seed oscillator and the MLO, the relative timing jitter and drift will be reduced substantially with a goal of 10 fs r.m.s. (Müller *et al.*, 2018). Preservation of low timing-drift and timing-jitter values from the seed oscillator through to the experiment is an important affair. The PP laser design therefore incorporates OBC (optical balanced cross-correlator) locking to compensate for drifts encountered in the laser up to the NOPAs, hence close to the output. Other systematic effects influencing pulse timing on the fs-scale can originate in the F-E pulse-picking accousto-optic modulators or the fact that the amplifiers are pumped in a transient fashion. These effects were either eliminated by design or are small for relevant burst lengths.

3. Pump–probe laser: summary of features and current performance

The PP laser was designed to work in four basic set points, determined by the intra-burst repetition rate settings of the F-E, which correspond to possible settings of the gun laser. Since both F-E and PA basically saturate in cw fashion for any of the possible repetition rates, the energy of a single pump pulse is inversely proportional to this repetition rate. Limited by nonlinearities, the lowest frequency setting is 100 kHz. During the R&D phase, repetition rates and NOPA configurations were tested as shown in Table 1. At SASE1, set points

1 and 2 have been commissioned and 2 is operated in user mode in compliance with FEL operation. Set points 3 and 4 are planned for commissioning during the upcoming shutdown in November–December 2018.

The choice of set point is determined by the required pulse energy or repetition rate. For both 800 nm and 1030 nm beams and, based on the set frequency, arbitrary patterns can then be programmed (PoD) down to single pulses. Setups for harmonic generation are available at the endstations.

The pulse durations accessible with the PP laser are listed in Table 2. The implemented NOPA scheme uses short pump pulses (<1 ps). This has the consequence that relatively simple means of dispersion tailoring (chirped mirrors or material dispersion) on the supercontinuum signal enables spectral selection with the pump pulse. Following some optimization, compressed pulse durations between 15 fs and around 300 fs are possible. These pulses are close to transform limited after compression, which is done with fused silica substrates in the beam delivery to the experiment in the 15 fs case. For longer pulses, the dispersion management is reversed and compression is achieved in the PP-laser hutch. At intermediate pulse durations, wavelengths between 750 nm and 850 nm (not tunable) can be configured.

It should be noted that changing these features comes at the cost of setup time, followed by transient behaviour, and hence will substantially reduce measurement time. Similar to changes of the PP laser set point, these changes should only be considered during setup days.

Finally, Figs. 4, 5 and 6 detail some of the PP laser pulse, beam and burst features as provided during recent experiments in May and August–September 2018 (set point 2).

4. Summary and outlook

We have described the PP laser specifically developed for the X-ray instruments at EuXFEL. Following the first installation of a production system and its successful user operation at FXE and SPB/SFX, all of the main development goals were reached, including (i) burst-mode operation, (ii) pulse durations of a few optical cycles to hundreds of fs, (iii) synchronized, low jitter/drift operation at repetition rates up to 4.5 MHz and (iv) pulse energies of a few µJ to tens of mJ. Some additional features include arbitrary pulse sequences (PoD), simultaneous laser operation at the FXE and SPB/SFX, dual wavelength beam

Table 2
The PP laser pulse durations and spectral widths.

Appropriate dispersion management on the NOPA signal enables a relatively large range of nearly transform-limited pulses at 800 nm. At medium long-pulse durations (50–300 fs), wavelengths around 800 nm can be set for operation (not tunable).

λ (nm)	Δτ	Δλ (nm)
1030	*ca.* 400 ps chirped	2
1030	850 fs	2
800	15 . . . 300 fs	90 . . . 4
750 . . . 850	50 fs	*ca.* 20

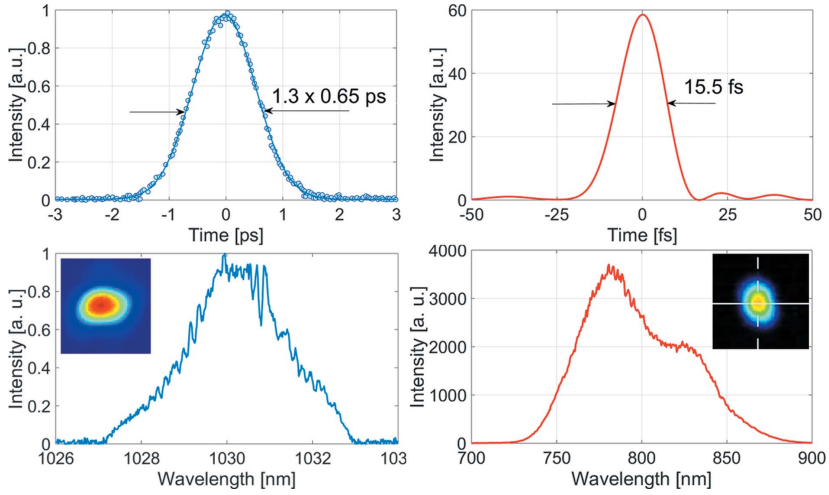

Figure 4
(Left) Autocorrelation and spectrum of the 1030 nm, 850 fs beam to FXE (blue). (Right) *SPIDER* trace and spectrum of the 800 nm, 15 fs beam to SPB/SFX (red). The insets show the far field of the respective beams. Both beams are nearly diffraction limited.

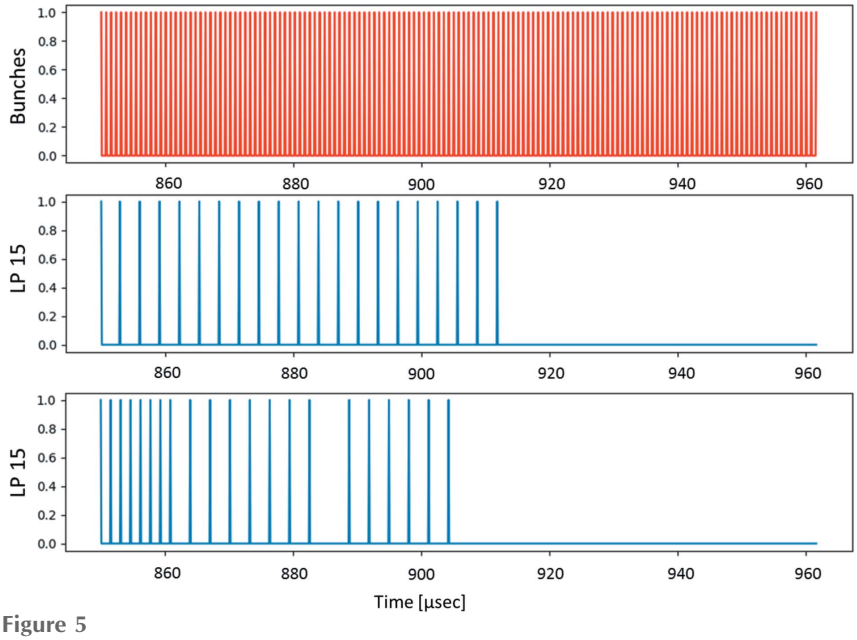

Figure 5
Three visualizations of the burst-pattern programming including the X-ray pattern at 1.1 MHz (red, top row), the programmed PP laser patterns down-picked to 275 kHz (blue, middle row) as used during FXE experiments and an example of an irregular pattern (blue, bottom row).

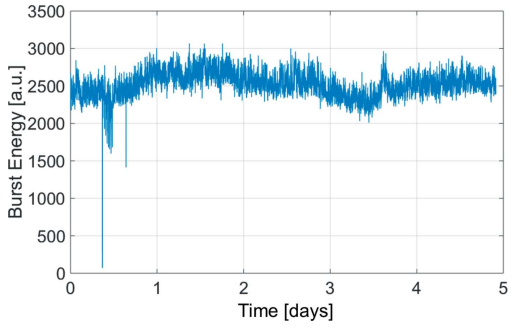

Figure 6
Five-day sample of the maximum pixel value of a CCD camera monitoring the beam shape (800 nm, 15 fs to SPB/SFX). This beam was provided for alignment and setup purposes. Incidences of lower signal levels (first day) mark requested changes in the burst pattern (down to single pulse).

delivery (800/1030 nm), and remote monitoring and control through Karabo. Experience from user operation at 1.1 MHz (determined by the EuXFEL accelerator) shows that the PP laser operates stably over the course of a five-day user run with power and far-field pointing remaining within 10% of nominal values, hence achieving very high up-times.

While these are considerable achievements, ongoing work is needed during the upcoming shutdown period in order to finalize commissioning of set points 3 and 4. This will make the highest possible pulse energies accessible and enable the use of a *TOPAS* parametric amplifier (TOPAS-Prime; http://www.lightcon.com/Product/TOPAS-Prime.html) for enhanced wavelength tuning. Another task concerns the activation of optical balanced cross-correlator sync-locking of the seeder, enhancing the jitter to expected values below 20 fs r.m.s. In cooperation with FXE and SPB/SFX, beam delivery to and characterization at the experiment will continue. Finally, ongoing development efforts aim at providing THz radiation for upcoming user runs.

In the spirit of a continuing improvement process, various possible upgrades and additional features are foreseen to be tested including: (i) increased Karabo integration to allow, for instance, automated procedures for change of shifts between FXE and SPB/SFX and time overlap finding; and (ii) alternating burst capability for instrument specific intra-burst repetition rates

Importantly, collection of long-term operation data and experience with the PP laser will allow maximizing of both up-time and flexibility for optimal user experience.

Acknowledgements

The authors would like to thank the FXE and SPB/SFX instrument teams for the fruitful and ongoing collaboration. We are grateful for the support provided by various technical groups at EuXFEL and DESY, which were pivotal to the success both in the development project as well as installation, commissioning and operation of the PP-laser at SASE1: R. Fabbri, G. Giovanetti, A. Silenzi, A. Parenti, H. Santos, and S. Brockhauser (Control and Analysis Software) J. Müller, S. Schulz, and C. Sydlo (Optical Synchronization) B. Fernandes, N. Coppola, and P. Gessler (Advanced Electronics) J. Szuba and K. Wrona (IT and Data Management) L. Wissmann (Electrical Engineering) G. Wellenreuther, A. Violante, and T. Haas (Facility Planning) P. Saffari, Z. Ansari, and S. Kozielski (Safety and Radiation Protection).

References

Altarelli, M. (2006). Editor. *The European X-ray FEL Technical Design Report*, DESY Report 2006–097. DESY, Hamburg, Germany.

Bressler, C., Biednov, M., Britz, A., Brockhauser, S., Frankenberger, P., Galler, A., Gawelda, W., Görries, D., Hauf, S., Khakhulin, D., Knoll, M., Korsch, T., Kubicek, K., Kuster, M., Lang, P., Lima, F. A., Schulz, S. & Zalden, P. (2019). *J. Synchrotron Rad.* **26**. Submitted.

Hauf, S., Heisen, B., Aplin, S., Beg, M., Bergemann, M., Bondar, V., Boukhelef, D., Danilevsky, C., Ehsan, W., Essenov, S., Fabbri, R., Flucke, G., Marsa, D. F., Goeries, D., Giovanetti, G., Hickin, D., Jarosiewicz, T., Kamil, E., Khakhulin, D., Klimovskaia, A., Kluyver, T., Kriri enko, Y., Kuhn, M., Maia, L., Mamchyk, D., Mariani, V., Mekinda, L., Michelat, T., Muennich, A., Padee, A., Parenti, A., Santos, H., Silenzi, A., Teichmann, M., Weger, K., Wiggins, J., Wrona, K., Xu, C., Youngman, C., Zhu, J., Fangohr, H. & Brockhauser, S. (2019). *J. Synchrotron Rad.* **26**. Submitted.

Mancuso, A. P., Aquila, A., Batchelor, L., Bean, R. J., Bean, R. J., Bielecki, J., Borchers, G., Doerner, K., Giewekemeyer, K., Graceffa, R., Kelsey, O. D., Kim, Y., Kirkwood, H. J., Legrand, A., Letrun, R., Manning, B., Morillo, L. L., Messerschmidt, M., Mills, G., Raabe, S., Reimers, N., Round, A., Sato, T., Schulz, J., Takem, C. S., Sikorski, M., Stern, S., Thute, P., Vagoivc, P., Weinhausen, B. & Tschentscher, T. (2019). *J. Synchrotron Rad.* **26**. Submitted.

Müller, J., Felber, M., Kozak, T., Lamb, T., Schulz, S., Sydlo, C., Titberidze, M., Zummack, F. & Schlarb, H. (2018). *Proceedings of the 29th Linear Accelerator Conference (LINAC2018)*, 16–21 September 2018, Beijing, China, pp. 988–993. MOPO121.

Pergament, M., Kellert, M., Kruse, K., Wang, J., Palmer, G., Wissmann, L., Wegner, U. & Lederer, M. J. (2014). *Opt. Express*, **22**, 22202–22210.

Pergament, M., Palmer, G., Kellert, M., Kruse, K., Wang, J., Wissmann, L., Wegner, U., Emons, M., Kane, D., Priebe, G., Venkatesan, S., Jezynski, T., Pallas, F. & Lederer, M. J. (2016). *Opt. Express*, **24**, 29349–29359.

Tschentscher, T., Bressler, C., Grünert, J., Madsen, A., Mancuso, A., Meyer, M., Scherz, A., Sinn, H. & Zastrau, U. (2017). *Appl. Sci.* **7**, 592.